Optical absorption in CdTe: d-core transitions

1991 J. Phys.: Condens. Matter 3 9041

(http://iopscience.iop.org/0953-8984/3/46/006)

J. Phys.: Condens. Matter 3 (1991) 9041–9053. Printed in the UK

Optical absorption in CdTe: d-core transitions

Roman Markowski and Marek Podgórny
Instytut Fizyki, Uniwersytet Jagielloński, 30-059 Kraków, ul. Reymonta 4, Poland

Received 3 September 1990, in final form 13 June 1991

Abstract. A self-consistent semirelativistic linear muffin-tin orbital calculation of the band structure is used in conjunction with the local-density approximation to derive the density of states and the direct interband contribution to the joint density of states for CdTe. The imaginary part of the dielectric function, $\varepsilon_2^{\flat}(\omega)$, is calculated with inclusion of the dipole transition matrix elements. A comparison is made with other theoretical and experimental results and an interpretation of the sharp structures in the absorption spectrum in the ultraviolet (UV) range is presented. The importance of the transitions from the Cd 4d states is carefully evaluated. It is shown that a very significant contribution to the imaginary part of the dielectric function in the UV range arises from the transitions originating in the upper part of the valence band to the higher conduction bands.

1. Introduction

The aim of this work is to present the self-consistent band structure for the zinc-blende-type semiconductor CdTe with special attention paid to the higher lying conduction bands and then to use the eigenvalues and eigenvectors to calculate the imaginary part of the dielectric function both in a constant matrix element approximation and with k-dependent matrix elements. The theoretical spectrum $\varepsilon_2^{\flat}$ will be presented and discussed in the energy range from about 10 to 20 eV. For this purpose we use the linear muffin-tin orbital (LMTO) approach in its scalar–relativistic form [1]. The procedure of the optical spectra calculation involves, as one of the steps, the self-consistent calculations of the electronic structure. CdTe is a 'canonical' II–VI semiconducting compound and its electronic structure has been studied several times in the past (see, e.g., [2–5], where a more extensive list of the earlier papers may be found). We have not yet attempted another standard calculation for its own sake. It is clear [6] that the electron correlation effects in semiconductors are not negligible and that the one-electron, local-density approximation (LDA) methods are not able to predict the correct energy gaps for semiconductors (this failure is described in the language of density functional theory as being caused by the discontinuity of the exchange–correlation energy when an electron is excited from the valence to the conduction band [7]. In a few recent papers, for example, [8], it has been shown that, despite this failure, the x-ray absorption spectra are essentially calculable within the LDA method. In this paper we attempt the LDA calculation of the near-UV spectrum for CdTe. The aim of the work is twofold:

(i) to resolve certain controversies concerning the interpretation of these spectra [9];
(ii) to shed some light on the applicability of the LDA scheme for such calculations.

0953-8984/91/469041 + 13 $03.50

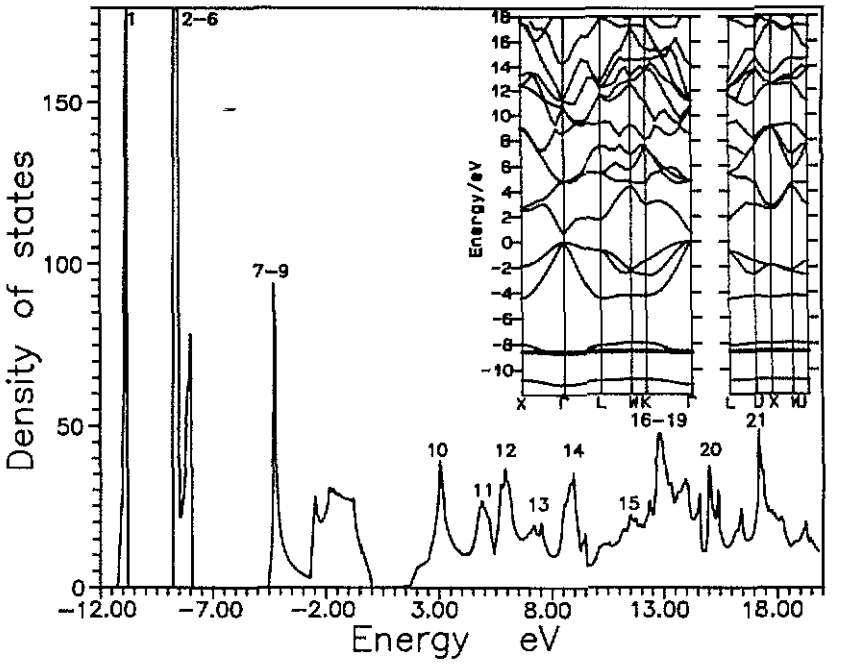

Figure 1. Total density of states of CdTe. Figures near the main peaks in the picture denote the serial numbers of the bands. In the inset the calculated band structure is shown.

In order to formulate such a diagnosis we remove from the calculational procedure another, hitherto very often used simplification, namely the constant matrix element approximation.

In the following we present the calculation of the imaginary part of the dielectric function ($\varepsilon_2^b(\omega)$) of CdTe and compare it with the experimental results [9]. We shall present the calculational methods in section 2, our results in section 3, the discussion in section 4 and the conclusions in section 5.

2. Method of calculation

In general, the calculation of the imaginary part of the dielectric function involves the following steps:

(a) self-consistent calculations of the band structure;
(b) calculation of the density of states and the Fermi level;
(c) calculation of the dipole transition matrix elements;
(d) calculation of the joint density of states and the imaginary part of the dielectric function itself.

All these steps have been carried out, as described below.

2.1. Electronic structure

The electronic structure of CdTe was calculated using the self-consistent LMTO method [1]. Scalar–relativistic (i.e. Darwin and mass–velocity) corrections as well as the 'combined correction term' [1, 10] were included in the calculation. The crystal structure was considered as an FCC lattice with four sites in the basis, Cd(0, 0, 0), Te($\frac{1}{4}, \frac{1}{4}, \frac{1}{4}$), E1 ($\frac{1}{2}, \frac{1}{2}, \frac{1}{2}$) and E2($\frac{3}{4}, \frac{3}{4}, \frac{3}{4}$), where E1 and E2 stand for 'empty spheres' [11] ($Z = 0$). The exchange–correlation LDA potential was used in the form proposed by Vosko *et al* [12]. The ratios of the atomic sphere radii for Cd, Te and empty spheres were taken as 1.25 : 1.25 : 1 : 1. Except for these ratios, an analogous scheme has been used by Cade and Lee [4] and by Alouani *et al* [5].

The self-consistent band structure of CdTe is presented in the inset of figure 1. All the calculations were carried out in a single energy panel, using 5s, 5p and 5d basis functions for Te and 5s, 5p and 4d functions for Cd, respectively. The total number of bands is equal to 36, the first nine of them being situated below the energy gap. We shall show that not only the Cd 4d states lying in -9 to -8 eV energy range but also the upper part of the valence band (-4.5 to 0.0 eV in figure 1) plays an important role in determining the absorption spectrum above 10 eV.

The shortcomings of the calculated band structure may be summarized as follows:

(a) the calculations do not include the spin–orbit coupling;

(b) the band structure agrees with experimental results in predicting CdTe to be a direct-gap semiconductor, but the gap is far too small (0.69 eV)—this is a standard feature of the band structures of semiconductors derived within the framework of the local-density approximation (LDA);

(c) the binding energies of the Cd 4d levels with respect to the top of the valence bands are too small ($\simeq$8.5 eV) and in disagreement with the experimental values ($\simeq$10.0 eV [13, 14]).

In table 1 we summarize the eigenvalues of several conduction states at some high-symmetry points and compare them with the results of a few other calculations. All the energies are in electron volts and are referred to the bottom of the conduction bands.

2.2. Density of states

With the use of the band structure the total density of states is calculated and presented in figure 1. We have also calculated the partial densities of states on each site and the main results are given in table 2, figures 2(*a*) and 2(*b*). We have used 12 divisions for ΓX and an energy step as small as 0.0023 Ryd. The zero of the energy scale in figures 1, 2(*a*) and 2(*b*) is at the top of the valence band.

2.3. Matrix elements

A complete calculation of the optical spectrum $\varepsilon_2^b(\omega)$ requires the computation of the dipolar matrix elements of the momentum operator $\boldsymbol{P} = \hbar\nabla/i$. In the full band calculations that provide both energy eigenvalues and eigenfunctions, it poses no special problem to compute the matrix elements at a given $\boldsymbol{k}$-point, although the task is numerically quite complex and the calculations rather time consuming.

The dipolar matrix elements $M_{if}^{k} = \langle f, \boldsymbol{k}|\, \boldsymbol{P}\, |i, \boldsymbol{k}\rangle$ are obtained from the scalar–relativistic self-consistent LMTO scheme. They are calculated with the wavefunction $|n, \boldsymbol{k}\rangle$

Table 1. Energy values (in eV) at some high-symmetry points of the Brillouin zone from band structure calculations (this work) compared with other theoretical and experimental determinations.

Level	Present calculation	Experiment[a]	Theory[b]
Γ_{6c}	0.00	0.00	0.00
L^1_{6c}	1.02	1.00[c]	1.23
X_{6c}	1.84	1.77	1.89
DOS peak	2.37	2.22	2.30[d]
Γ_{7c}	4.13	3.80	3.77
Γ_{8c}	4.13		4.02
L^2_{6c}	4.73	4.45[c]	4.59
$L_{4.5c}$	4.73	4.82[c]	4.76
X_{7c}	2.10		2.36
Fundamental gap	0.69	1.59	
Cd 4d threshold	9.20	11.59 ± 0.05	

[a] From table 2 of [9].
[b] From table 2 of [9] and from table 21 of [2].
[c] From table 2 of [9] and from [2, 25, 26, 27, 28].
[d] From figure 2 of [24].

expressed in terms of the one-centre expansion [1]. It is a relatively easy matter to calculate the k-dependent matrix elements if one makes use of the Wigner–Eckart theorem for the gradient formula [15].

In the case of LMTO because of the nature of the orbitals constructed the intersite transitions do not exist and hence the method of calculation becomes rather straightforward [16, 17]. In the present study we have fully implemented the computational scheme devised by Koenig and Khan [16] and by Alouani *et al* [17].

2.4. Optical absorption

The optical absorption is proportional to the imaginary part of the dielectric function $\varepsilon(\omega, q)$ with $q \simeq 0$ in the optical range. In the limit of vanishing linewidth the interband transition $\varepsilon_2^b(\omega)$ contribution of the dielectric function is given by [5, 18]:

$$\varepsilon_2^b(\omega) = \frac{4\pi^2 e^2}{3m^2\omega^2} \sum_i \sum_f \int_{BZ} \frac{2}{(2\pi)^3} d^3k \, |M_{if}^k|^2 \, \delta(E_f^k - E_i^k - \hbar\omega) f_f^k (1 - f_i^k) \qquad (1)$$

where E_i^k and E_f^k are the occupied and empty states, respectively, at a given k-vector, f_n^k is the zero-temperature Fermi distribution function for the state $|n, k\rangle$ with band index n and wavevector k.

The integration of equation (1) over k-space is performed by the tetrahedron method [19] based on 240 k-points in the irreducible part of the Brillouin zone (IBZ). We calculate the dipole matrix elements at the four corners of each tetrahedron and use their arithmetic average during the integration.

The imaginary part of ε, $\varepsilon_2^b(\omega)$, is calculated for the photon energy ranging up to 20 eV. The dielectric function for CdTe without any lifetime broadening is shown in figure 3.

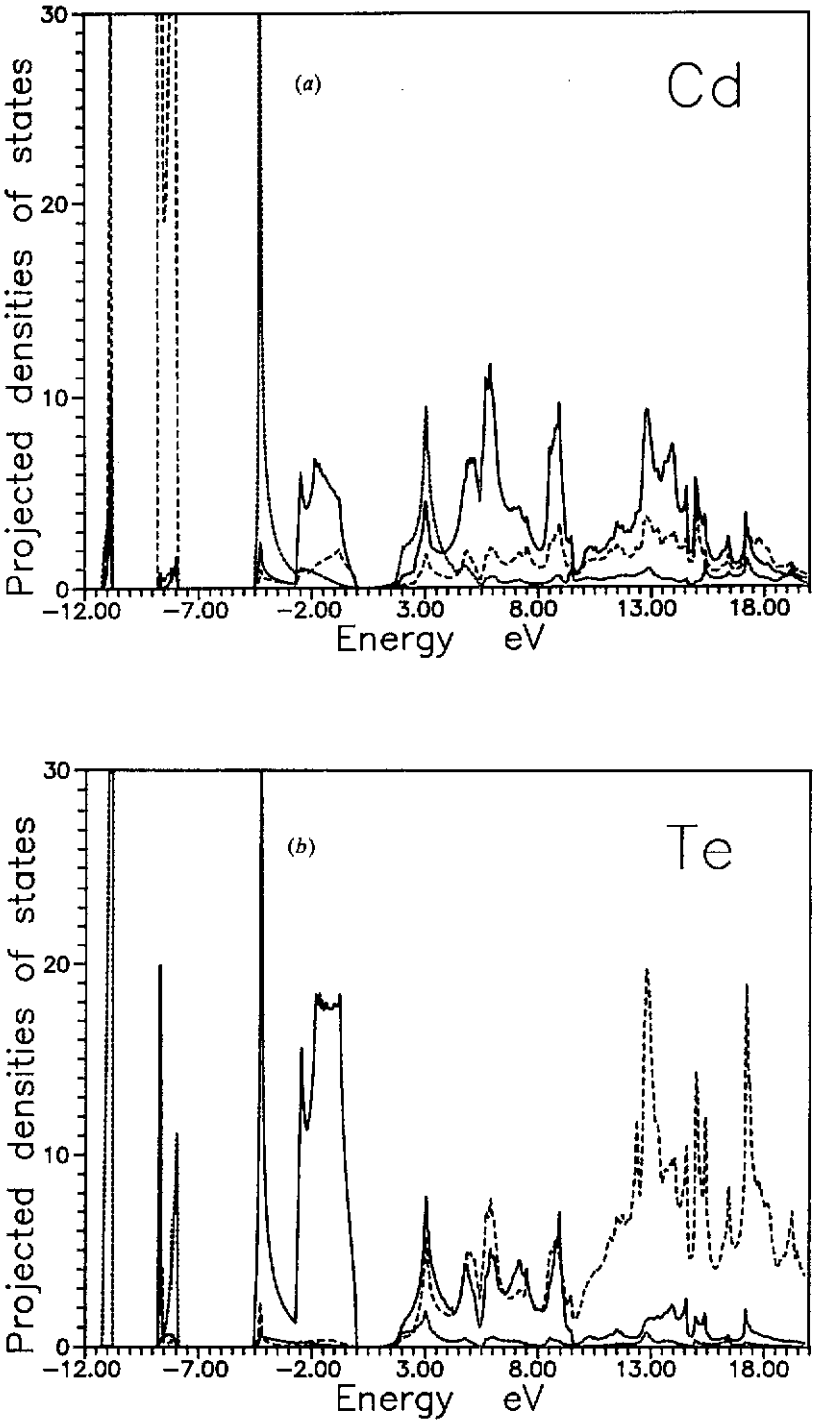

Figure 2. (*a*) Partial densities of states at a Cd site: broken curve (short dashes), s-projected DOS; full curve, p-projected DOS; broken curve (long dashes), d-projected DOS. (*b*) Partial densities of states at a Te site: broken curve (short dashes), s-projected DOS; full curve, p-projected DOS; broken curve (long dashes), d-projected DOS.

Table 2. Number of electrons N below the Fermi level of different sites and the intersite charge transfer (in electronic units) that gives an ionic character to the atomic sites.

	N_s	N_p	N_d	Q
Cd	0.92	1.02	10.00	−0.05
Te	1.74	3.52	0.15	−0.59
E1	0.15	0.15	0.06	0.36
E2	0.12	0.12	0.04	0.28

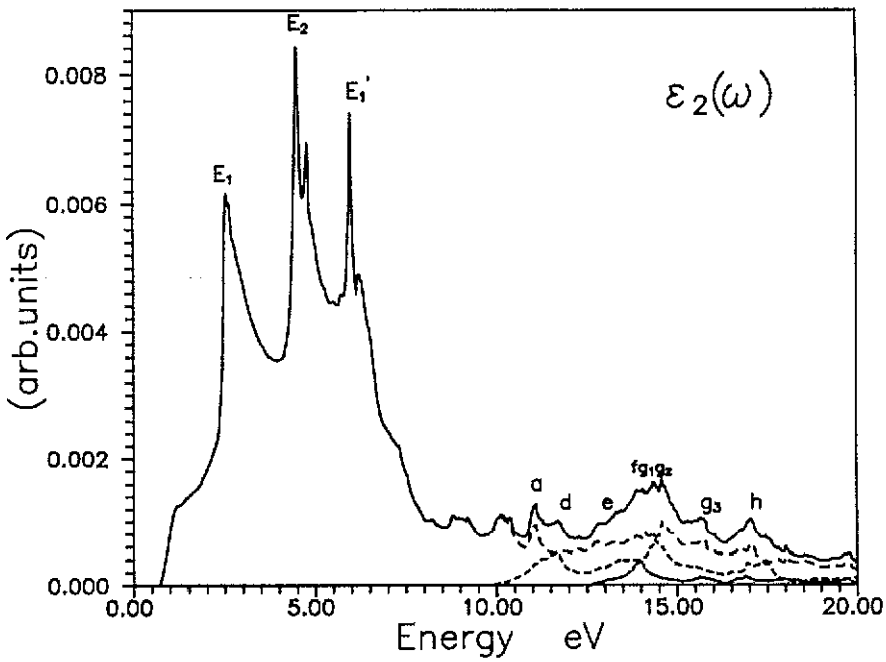

Figure 3. Imaginary part, $\varepsilon_2^b(\omega)$, of the dielectric function of CdTe (full curve). The broken curve (short dashes) represents the contribution of band 1, the broken curve (medium length dashes), the contribution from the bands 2 to 6, and the broken curve (long dashes), the contribution of the bands 7 to 9.

There are four curves displayed in figure 3. The broken curve (short dashes) represents the contribution to the imaginary part $\varepsilon_2^b(\omega)$ being the result of the transitions from the first band to the bands lying above the Fermi level (bands 10, 11, etc). The contribution originating from the bands lying in the energy range −9 to −8 eV (bands 2 to 6) is represented by the broken curve (medium length dashes). The broken curve (long dashes) describes the transitions from bands 7, 8 and 9 (valence bands). Finally, the total imaginary part $\varepsilon_2^b(\omega)$ of the dielectric function is represented by the full line.

When the matrix elements are assumed to be constant, the resulting quantity is proportional to the unbroadened joint density of states in which the selection rules are completely ignored. This function and its contributions (divided by ω^2) are displayed in figure 4. It is important to note that whereas in the visible and near-UV range the constant

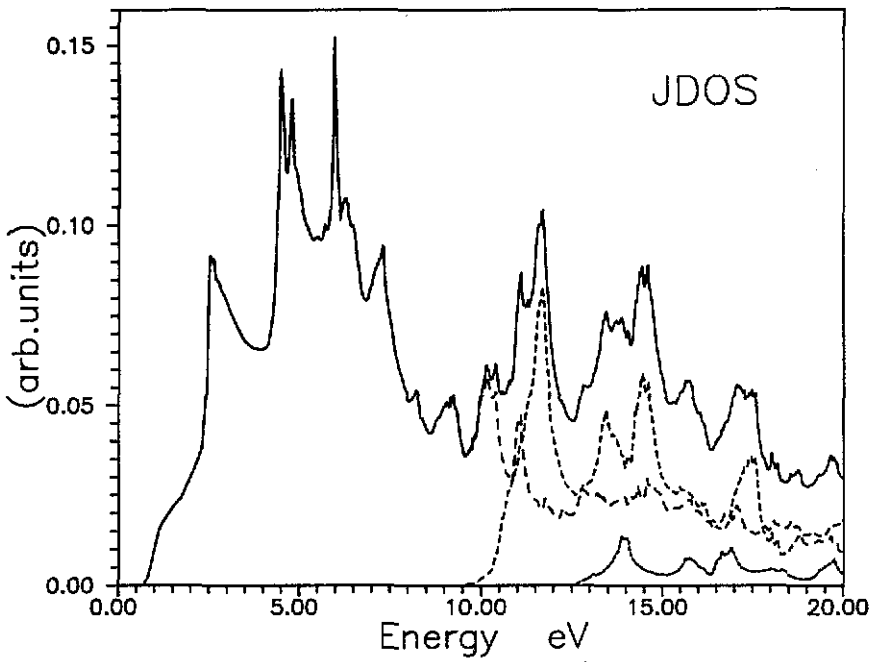

Figure 4. Joint density of states divided by ω^2 (JDOS) (full curve). The broken curve (short dashes) represents the contribution of band 1, the broken curve (medium length dashes) the contribution of bands 2 to 6 and the broken curve (long dashes) the contribution of bands 7 to 9.

matrix element approximation seems to be reasonable, it fails utterly when the high-energy part of spectrum is included. The selection rules damp this part of ε_2^b by a factor of about four as compared with the JDOS spectrum.

3. Results of calculation

The imaginary part of the dielectric function between 0 and 20 eV for CdTe is shown in figure 3. The positions of all the peaks in $\varepsilon_2^b(\omega)$ in comparison with the experiment and other (adjusted) calculations are given in table 3.

In table 4 we list the energy gaps at some critical points in comparison with the results from Chelikowsky and Cohen's EPM calculation [2] and the Alouani *et al* [5] LMTO calculations. In order to compensate for the gap values that are too low Alouani *et al* [5] applied *ad hoc* the 'false Darwin shifts' by means of extra sharply peaked potential at the nuclei.

The LDA is known to fail in predicting a correct fundamental energy gap for semiconductors (tables 3 and 4). It is also seen (figure 3), that the main structures E_1 and E_2 in $\varepsilon_2^b(\omega)$ are located too low in energy when compared with experiment. This is a common feature of band structures derived within the LDA, that all peaks in the spectrum $\varepsilon_2^b(\omega)$ are located at too low an energy. Furthermore, the binding energy of Cd 4d states is too small when compared with experimental values ([13, 14], table 1). This causes an

Table 3. Experimental and theoretical values (in eV) of energy gaps in CdTe compared with the LDA values calculated in the present work.

Peak	Experiment	Other calculations	Present calculations	
			unadjusted	adjusted
E_0	1.59 [29]	1.51 [5]	0.69	1.56
	1.43 [30]			
	1.50 [31, 32]			
E_1	3.30 [31]	3.16 [5]	2.54	3.37
	3.44 [33]			
	3.35 [32]			
E_2	5.00 [32]	4.83 [5]	4.50	5.20
	5.40 [9]		4.80	5.51
E_1'	6.79 [9]	5.76 [5]	5.98	6.71
a	12.17 [9]		11.10	12.10
c	13.36 [9]			13.30
d	13.81 [9]		11.68	13.85
e	15.4 [9]		13.27	15.60
f	16.0 [9]		13.87	16.00
g	17.1 [9]		14.32	16.40[a]
			14.58	16.70[a]
			15.64	18.00[a]
h	19.0 [9]		17.01	18.8[a]
				19.6[a]

[a] See figure 5.

Table 4. Energy gaps (in eV) at some critical points in comparison with the empirical pseudopotential method (EPM) [2] and the LMTO results [5].

	EPM	LMTO	Present calculation	
			unadjusted	adjusted
Γ_6^c–Γ_8^v	1.59	1.51	0.69	1.56
L_6^c–$L_{4,5}^v$	3.47	2.92	2.44	3.46
L_6^c–L_6^v	4.00	3.45	2.44	3.46
X_6^c–X_7^v	5.08	4.63	4.39	5.10
X_6^c–X_6^v	5.46	4.96	4.39	5.10

additional shift towards the lower energies of the sharp structures originating in the metal (Cd) uppermost d levels on the $\varepsilon_2^b(\omega)$ spectrum (figure 3).

A procedure is therefore needed which aligns the experimental and theoretical energy scales. An *'ab initio'* alignment of the energy scales is not possible because our calculations of the electronic structures deliver false information about the energy gaps and no information at all about the chemical shifts. We have therefore adopted the following approach: the discrepancy between the observed and calculated binding energies of the semicore Cd 4d states is a correlation effect, which is mainly the result of the change of occupancy of the Cd 4d level in the excitation process. The experimental binding energy is known from photoemission experiments. Since there is no reason to

expect that the correlation shift will be much different in the process of optical excitation, the experimental value of binding energy of these states was introduced into the LMTO procedure by changing the potential parameters ($E_d \rightarrow E_d - 1.2$ eV), and the full calculation of band structure was performed once more. Furthermore, we have observed that one can bring into fair agreement the experimental and calculated positions of the E_0, E_1 and E_2 maxima shifting the $\varepsilon_2^b(\omega)$ uniformly by about 0.9 eV. This amounts to the rigid shift of the conduction bands by 0.9 eV, which is precisely the difference between the calculated and experimental energy gap. In the following, we refer to the 'adjusted spectrum', which results from both operations described above.

We did not use the 'false Darwin shifts' procedure devised by Christensen [20] and used by Alouani *et al* [5]. Although this procedure has a touch of sophistication, we think that there is no physical justification for its usage whatsoever. It actually corrects the fundamental gap value, which is too low, but for higher energies it influences the band energies in an unpredictable way that depends on the degree of the s–p mixing for the *k*-points away from the Brillouin zone centre. Our simple procedure of energy scale alignment is perhaps trivial but its physical background is much more transparent than that of the 'false Darwin shift' procedure—it assumes simply that the LDA errors arising from the potential discontinuity are independent of the final energy of the excited electron. This effect is, however, taken into account later by using the energy-dependent lifetime broadening of the calculated optical spectrum (see below). Of course we have to remember that the LDA band structure is not only in error by a constant shift of the conduction bands; the dispersion may also be wrong [21]. The result of the alignment procedure is presented in figure 5 as well as in tables 3 and 4. In the following we shall try to show that, under the enumerated assumptions, a consistent interpretation of the UV spectra of CdTe is possible.

4. Discussion

The unadjusted absorption spectrum of CdTe is presented in figure 3. It consists of two distinct spectral regions. The onset of the absorption edge in the unadjusted $\varepsilon_2^b(\omega)$ spectrum occurs at 0.69 eV. The low-energy region, extending approximately to 10 eV is characterized by a rather high, strong structure. The optical transitions associated with the structures up to about 8 eV have been studied in detail by several authors (see [9] for a more detailed reference list). The most important contribution to the peaks E_1 and E_2 arises from the transitions from the uppermost valence band to the first conduction band throughout the large volume of the Brillouin zone.

In order to illustrate the effects of the matrix elements we should compare the imaginary part of the dielectric function $\varepsilon_2^b(\omega)$ calculated with inclusion of the transition matrix elements (figure 3) and the joint density of states function divided by ω^2 (figure 4). The peaks present in the JDOS at high energy are reduced significantly (as has already been discussed in [5]) in the $\varepsilon_2^b(\omega)$ spectrum because the transition probability becomes small at high energy. Hence, a quantitative comparison with experiment is only meaningful if the matrix elements of the *P*-operator are included in the calculation of the $\varepsilon_2^b(\omega)$ spectrum.

At higher energies a wealth of sharp features appear in the CdTe absorption spectrum (figure 3). In our work we have studied the origins of the structures labelled a, c, d, e, f, g_1, g_2, g_3 and h (figure 6), which are situated in the energy region between 10 and 20 eV.

The unadjusted and adjusted spectra for $\varepsilon_2^b(\omega)$ on an expanded scale (in the region of the d excitations) are presented at figures 5 and 6, respectively. The broken curve

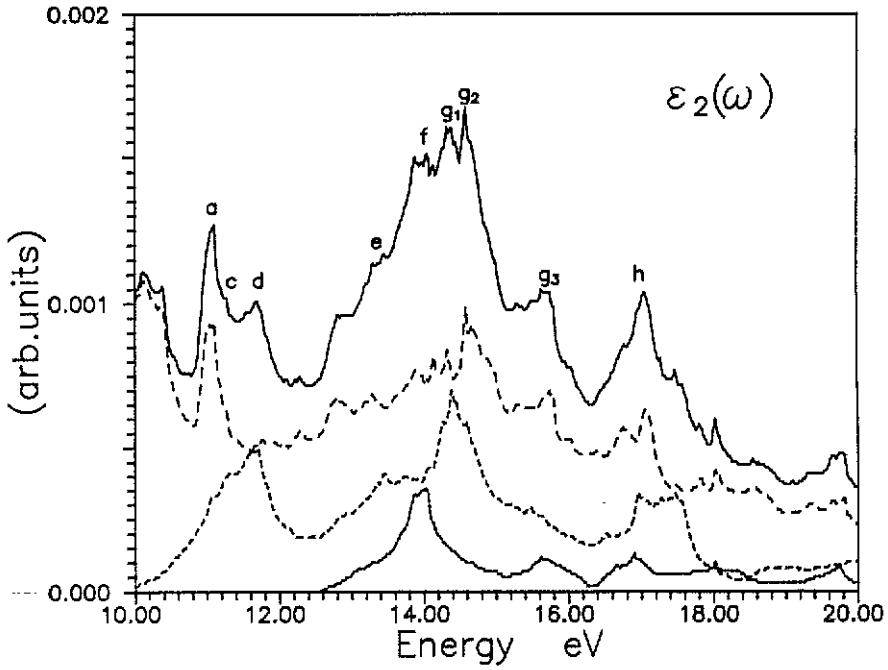

Figure 5. Absorption spectrum $\varepsilon_2^b(\omega)$ in the region of the cation d excitations (unadjusted case). The broken curve (short dashes) represents the contribution of band 1, the broken curve (medium length dashes) the contribution of bands 2 to 6, the broken curve (long dashes) the contribution of bands 7 to 9 and the full curve represents the total absorption spectrum.

(short dashes) represents the contribution to the imaginary part $\varepsilon_2^b(\omega)$ which derives from transitions from the first band (Te 5s) to the bands lying above the Fermi level. In that part of the spectrum three peaks at 14.02, 15.62 and 16.90 eV are found near the f, g_3 and h positions, respectively. The most important contribution to these three peaks arises from the transitions from the first band to the tenth, eleventh and the twelfth and thirteenth bands in the Te sphere, respectively. The expectation [9] that the transitions from the Te 5s yield structures that are much broader than those from the metal d states and mainly contribute a smooth background to the absorption spectrum turns out to be false. This notion concerns especially the first peak at 14.02 eV. The peak positions and their relative heights fit well with the partial density of states for the Te site (figure 2(*b*)).

The broken curve (medium length dashes) represents the contribution of transitions originating in the metal Cd 4d levels. The onset of the absorption contribution occurs at 9.9 eV. The contribution is characterized by five sharp peaks at 11.68, 13.44, 14.60, 16.96 and 17.46 eV near the d, e, g_1 and h positions, which arises from the transitions D → 10, D → 11, D → 12, 13 and D → 14, respectively (D denotes the Cd 4d states—it refers to bands 2 to 6). The picture is in agreement with the partial densities of states on the Cd site (figure 2(*a*)) if we take into account the positions and the relative heights of the peaks. If we compare figures 3 and 4 we can observe the strong influence of the transition matrix elements on the Cd 4d contribution.

The broken curve (long dashes) represents the contribution to $\varepsilon_2^b(\omega)$ originating in the uppermost three valence bands (namely bands 7, 8 and 9). Essentially, there are two

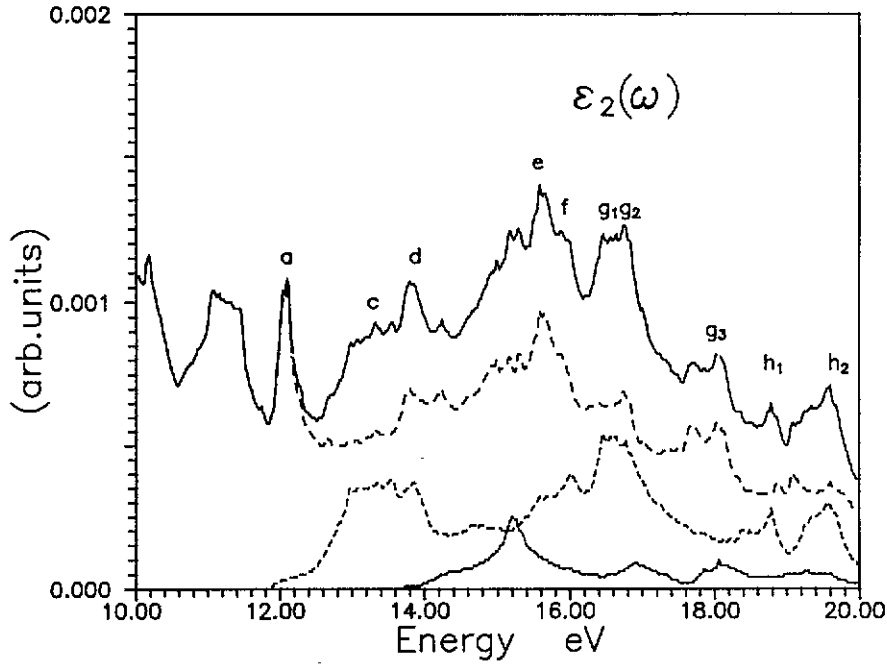

Figure 6. The absorption spectrum $\varepsilon_2^b(\omega)$ in the region of the cation d excitations (adjusted case). The broken curve (short dashes) represents the contribution of band 1, the broken curve (medium length dashes) the contribution of bands 2 to 6, the broken curve (long dashes) the contribution of bands 7 to 9 and the full curve represents the total absorption spectrum. The assignments of the observed structures are also included.

structures: the first sharp peak at 11.10 eV arises from the transition from band 8 to band 14 at the Te site; the second broad peak is centred at 14.58 eV and is created by transitions from bands 7, 8 and 9 to bands 15 to 19 at the Te site. The shape of the line is consistent with the partial density of states for Te (figure 2(*b*)).

We have attempted to compare our theoretical result (full curve, figure 6) with the experimental study of the reflectivity of CdTe presented in paper [9]. The comparison is difficult, as mentioned above, because of several problems.

(a) The fundamental gap is too low (table 1): all peaks in figure 5 are shifted towards lower energies about 0.9 eV.

(b) The Cd 4d bands are too high with respect to the maximum of the valence band (table 1): the sharp structures above approximately 10 eV originating in the uppermost Cd d levels are shifted additionally by about 1.2 eV towards lower energies.

(c) The calculations do not include the spin–orbit coupling so that the number of interband contributions is reduced.

Furthermore, our results use one-electron calculations, so that observed deviations from the experimental amplitudes and peak positions might be attributed to many-body effects.

In the discussion presented so far it has been assumed that the initial and final states have infinite lifetimes and thus that their natural widths are zero. So $\varepsilon_2^b(\omega)$ depicted in

figure 6 was calculated without inclusion of the effects of the finite relaxation time (many-body and excitonic effects). In addition, surface and screening effects may influence the peak heights in the experimental spectrum [5].

It is found experimentally that the initial and final states do have finite lifetimes [22]. These finite lifetimes imply a Lorentzian line shape of the initial and final states which manifests itself as a broadening of the spectra. This effect can be incorporated in the single-particle results by convoluting them with a Lorentzian function of a width that depends on the final-state energy (which increases significantly with the energy of the final state). We should also take into account the experimental resolution in the Gaussian form:

$$\tilde{\varepsilon}_2^{\mathrm{b}}(E) = \frac{1}{(2\pi)^{1/2}\Gamma} \int \exp\left(-\frac{(E-E')^2}{2\Gamma^2}\right) \varepsilon_2^{\mathrm{b}}(E')\,\mathrm{d}E'.$$

It is known, that the LMTO method cannot reliably describe bands positioned higher than 1–2 Ryd above V_{MTZ}, where V_{MTZ} is the average interstitial potential. In our calculation we limited the energy range considered to approximately 20 eV above the valence band maximum, that is up to 2.2 Ryd above V_{MTZ}. Hence, we should expect that the contribution of the broken curve (long dashes) to $\varepsilon_2^{\mathrm{b}}(\omega)$ depicted in figure 5 is more uncertain than the other contributions.

In the interpretation of the optical spectrum above 10 eV we concentrate on the structures associated with the excitation of the Cd 4d levels. The theoretical, adjusted spectrum of $\varepsilon_2^{\mathrm{b}}(\omega)$ (description of the alignment procedure above) is characterized by a first sharp peak (a) at 12.10 eV followed by structures labelled c, d, e, f, g_1, g_2, g_3 and h, respectively (figure 6, table 3).

The peaks c and d can be associated with transitions from the Cd 4d levels to the first conduction band (band 10). The peaks f, g_1 and g_2 can be interpreted as the transitions from the Te 5s levels to the first conduction band and from the Cd 4d levels to the second conduction band (band 11).

The peak g_3 arises from transitions from Cd 4d levels to the bands 12 and 13.

The agreement with the experimental results and the discussion presented in [9] is quite satisfactory. The largest discrepancy is found in the interpretation of the peak 'a' in the $\varepsilon_2^{\mathrm{b}}(\omega)$ spectrum. The suggestion that the peak a of the CdTe spectrum is a core excitation [9, 23] seems to be in error. We interpret this sharp peak as a transition from the eighth to the fourteenth band.

5. Conclusions and summary

A self-consistent band structure for CdTe is obtained using the LMTO method. The outcome of this calculation is used to derive the density of states and the imaginary part of the dielectric function. The UV range of the dielectric function is calculated for the first time.

Contrary to common belief, apart from the strong contribution from the Cd 4d states transitions, we find in this energy range a very significant contribution of the transitions originating in the upper part of the valence band to the higher conduction bands.

In the method of calculation presented above it is easy to determine the regions in k-space giving the major contributions to the intensity of the peaks of the $\varepsilon_2^{\mathrm{b}}(\omega)$ spectrum. To allow a direct comparison between theory and experiment, an 'alignment procedure' is suggested and applied. The adjusted theoretical spectrum is directly compared with

experimental results above 10 eV. In general, our calculations allow for a consistent assignment of the structures in the experimental reflectivity spectrum for CdTe. This supports the conjecture that for II–VI semiconductors the corrections to LDA resulting from the discontinuity of the exchange–correlation energy should depend rather weakly on the energy.

Acknowledgment

We are grateful to Professor A Kisiel for suggesting this work and for many stimulating discussions.

References

[1] Andersen O K 1975 *Phys. Rev.* B **12** 3060
[2] Chelikowsky R and Cohen M L 1976 *Phys. Rev.* B **14** 556
[3] Czyżyk M T and Podgórny M 1980 *Phys. Status Solidi* b **98** 507
[4] Cade N A and Lee P M 1985 *Solid State Commun.* **56** 637
[5] Alouani M, Brey L and Christensen N E 1988 *Phys. Rev.* B **37** 1167
[6] Krüger P, Wolfgarten G and Pollmann J 1985 *Solid State Commun.* **53** 885
[7] Perdew J P and Levy M 1983 *Phys. Rev. Lett.* **51** 1884
Sham L J and Schlüter M 1983 *Phys. Rev. Lett.* **51** 1888
[8] Kisiel A, Dalba G, Fornasini P, Podgórny M, Olcszkiewicz J, Rocca F and Burattini E 1989 *Phys. Rev.* B **39** 7895
[9] Kisiel A, Zimnal-Starnawska M, Antonangeli F, Piacentini M and Zema N 1986 *Nuovo Cim.* **8** D 436
[10] Skriver H L 1984 *The LMTO Method (Springer Series in Solid State Sciences 41)* (Berlin: Springer) p 95
[11] Jarlborg T and Freeman A J 1979 *Phys. Lett.* **74A** 399
[12] Vosko S H, Wilk L and Nusair M 1980 *Can. J. Phys.* **58** 1200
[13] Eastman D E, Grobman W D, Freeouf J L and Erbudak M 1974 *Phys. Rev.* B **9** 3473
[14] Taniguchi M, Ley L, Johnson R L, Ghijsen J and Cardona M 1986 *Phys. Rev.* B **33** 1206
[15] Edmonds A R 1974 *Angular Momentum in Quantum Mechanics* (Princeton, NJ: Princeton University Press) p 79
[16] Koenig C and Khan M A 1983 *Phys. Rev.* B **27** 6129
[17] Alouani M, Koch J M and Khan M A 1986 *J. Phys. F: Met. Phys.* **16** 473
[18] Szmulkowicz F and Segall B 1981 *Phys. Rev.* B **24** 892
[19] Lehman G and Taut M 1972 *Phys. Status Solidi* b **54** 469
[20] Christensen N E 1984 *Phys. Rev.* B **30** 5753
[21] Bachelet G and Christensen N E 1985 *Phys. Rev.* B **31** 879
[22] Müller J E and Wilkins J W 1984 *Phys. Rev.* B **29** 4331
[23] Aspnes D E, Olson C G and Lynch D W 1975 *Phys. Rev.* B **12** 2527
[24] Au-Ban Shen and Sher A 1982 *J. Vac. Sci. Technol.* **21** 138
[25] Chadi D J, Walter P J, Cohen M L, Petroff Y and Balkanski M 1972 *Phys. Rev.* B **5** 3058
[26] Walter J P, Cohen M L, Petroff Y and Balkanski M 1970 *Phys. Rev.* B **1** 2661
[27] Rodzik A and Kisiel A 1983 *J. Phys. C: Solid State Phys.* **16** 203
[28] Ley L, Pollak R A, McFeely F R, Kowalczyk S P and Shirley D A 1974 *Phys. Rev.* B **9** 600
[29] Thomas D G 1961 *J. Appl. Phys.* **32** 939
[30] Yamada S 1960 *J. Phys. Soc. Japan* **15** 1940
[31] Mei J R and Lemos V 1984 *Solid State Commun.* **52** 785
[32] Lautenschlager P, Logothetidis S, Vina L and Cardona M 1985 *Phys. Rev.* B **32** 3811
[33] Cardona M and Greenaway D L 1963 *Phys. Rev.* **131** 1009